

RESEARCH ARTICLE

Open Access



# The microstructure of multicolor hare's fur glaze: the correlation between morphological and compositional characteristics and glaze color

Ming Guan<sup>1</sup>, Baoqiang Kang<sup>1</sup>, Xiangjun Wei<sup>2\*</sup>, Gen Li<sup>1</sup>, Cui Jia<sup>1</sup>, He Li<sup>1</sup>, Yinzong Ding<sup>1</sup> and Yong Lei<sup>1\*</sup>

## Abstract

The hare's fur glazed Jian wares characterized by radial fur-like strips, as one of the typical representatives of Chinese ceramics in the 10th-13th century (A.D.), were famous for the aesthetic values in highlighting the color sparkling effects of tea soup, which were one of the indispensable tea wares in tea culture. The firing technology of hare's fur glaze of Jian wares not only played a crucial role in the development of Chinese ceramic history, but also enlightened the modern imitation technology. The hare's fur glaze of Jian wares can be further grouped according to the color of strips, of which the yellowish-brown hare's fur glaze (yellowish-brown matte strips), gold hare's fur glaze (golden shiny strips) and silver hare's fur glaze (bright silvery strips) were the most representative types. Epsilon- $\text{Fe}_2\text{O}_3$ , a specific metastable crystal phase, has become a research hotspot as the chromogenic crystals of hare's fur glaze, however, the comparative analysis focused on the correlation between  $\epsilon\text{-Fe}_2\text{O}_3$  and the macroscopic glaze color has been barely reported. In our work, the bright color strips (hare's fur area) and black strips (black glaze area) of silver, gold and yellowish-brown hare's fur glaze were morphologically and compositionally analyzed by SEM and EDS, respectively. The morphological features and compositional differences of three representative types of hare's fur glaze samples were summarized, which indicated the differences in the size, distribution and coverage of crystals and the distribution and contents of materials. It was speculated that high-level of  $\text{Fe}_2\text{O}_3$  and CaO with low-level of  $\text{SiO}_2$  and  $\text{Al}_2\text{O}_3$  may relate to the crystallization of  $\epsilon\text{-Fe}_2\text{O}_3$ . This work helps in laying the foundation of further explanation of the technological differences of hare's fur glazes.

**Keywords:** Hare's fur glaze, Jian wares, SEM, EDS

## Introduction

The glossy black-brown glazed porcelain was one of the representative types of Chinese ceramics, which occupied a unique place in Chinese ceramic history, especially in the culturally prosperous Song Dynasty (the 10th-13th century A.D.) reflecting the pursuit of simplicity and elegance. Of all the black-brown glazed porcelains, the hare's fur glaze was considered as the superior quality

and the most popular type, which was known for the radial strips shaped as the fur of hare. The hare's fur glaze was also famous for the aesthetic values in highlighting the white color and the sparkling effects of tea soup due to the intensive color comparison, which made it an optimal container in tea culture [1]. As the most famous product of Jian kiln, Jian wares were acknowledged as the most typical representatives of the hare's fur glaze, which not only occupied the most crucial role in the black-brown glaze development in Chinese ceramic history, but also profoundly affected the Asian ceramic history, especially for Japanese ceramics [2]. The firing technology of

\*Correspondence: weixiangjun@sinap.ac.cn; leiyongleo@hotmail.com

<sup>1</sup> The Palace Museum, Beijing, China

<sup>2</sup> Shanghai Advanced Research Institute, Shanghai Synchrotron Radiation Facility, Chinese Academy of Sciences, Shanghai, China

hare's fur glazed Jian wares also enlightened the modern imitation technology of hare's fur glaze [3].

The hare's fur glaze of Jian wares can be further grouped based on the color of strips, of which the yellowish-brown hare's fur glaze, gold hare's fur glaze and silver hare's fur glaze were the most representative types. In the previous study, Chen et al. proposed the scientific category criteria of the three types of hare's fur glaze based on the comparison of the samples from Luhuping kiln based on stereoscopic microscope [4]. Specifically, [1] the yellowish-brown hare's fur glaze was characterized by matte yellowish-brown strips with the largest number of samples; [2] the gold hare's fur glaze had golden yellow strips which shined golden gloss with certain samples; [3] the silver hare's fur glaze was characterized by vaporous white strips or bright silver strips with shine without obvious crystallization on the glaze surface, the quantity of which was extremely rare. The multiple types of hare's fur glaze reflected the perfect aesthetical pursuit of tea wares, among which the silver hare's fur glaze with silvery and radial strips were the most acclaimed type since the silvery streaks perfectly presented the sparkling tea soup. The admiration and status of silver hare's fur glaze could be caught a glimpse from the "*Da Guan Cha Lun*" written by the emperor *Huizong* of Song Dynasty (A.D. 1082–1135). However, due to the difficulty of firing process and low yield, the extant amount of hare's fur glazed Jian wares samples was scarce, especially for the silver hare's fur glaze, resulting in the lack of responding researches [4].

The surface crystallization on the iron-rich porcelain glaze, including the dendritic microstructure of iron oxides, has been widely studied in historical sherds and imitations in recent years [5–8]. Interestingly, epsilon- $\text{Fe}_2\text{O}_3$  ( $\epsilon\text{-Fe}_2\text{O}_3$ ), a specific metastable crystalline polymorph of iron oxide [9], has become a research hotspot as the chromogenic crystals of sauce, oil spot, and hare's fur glazes [10–13]. As a promising magnetic material,  $\epsilon\text{-Fe}_2\text{O}_3$  has been limited in application due to the difficulty in modern chemical synthesis [14–16]. However, as early as the 7th–10th century of ancient China,  $\epsilon\text{-Fe}_2\text{O}_3$  was successfully synthesized on the colored glaze of Changsha kiln [17], which was successively reported the existence in the brown glaze of Yaozhou kiln of Northern Song Dynasty (the 10th–12th century A.D.) [11], the sauce glaze of Qilizhen kiln of Southern Song Dynasty (the 12th–13th century A.D.) [18], the hare's fur glaze and oil spot glaze of Southern Song Dynasty [19, 20], the hare's fur glaze of Jizhou kiln [21], and the purple-gold glaze of Qing Dynasty (the 17th–20th century A.D.) [22]. However, the existing researches were mostly focused on one type of glaze or the comparison of glazes in different kilns [23], lacking the comparatively studies emphasized

on the correlation between the microscopic structures of  $\epsilon\text{-Fe}_2\text{O}_3$  and the macroscopic glaze color, since  $\epsilon\text{-Fe}_2\text{O}_3$  was found on the golden, silvery and brownish glazes in one kiln. The comparison of  $\epsilon\text{-Fe}_2\text{O}_3$ -rich glaze in different types of hare's fur glazed Jian wares unearthed from Shuiji kiln was expected to provide enlightenment for the controllable synthesizing method for specific  $\epsilon\text{-Fe}_2\text{O}_3$  crystals and other corresponding researches.

In this work, the bright color strips (hare's fur area) and black strips (black glaze area) of three representative types of hare's fur glaze samples (silver, gold and yellowish-brown) were compared. The microstructures of the hare's fur area and black glaze area in different types of samples were visualized based on scanning electron microscope (SEM). Besides, energy dispersive spectroscopy (EDS) was applied for elemental imaging microanalysis and semi-quantitative analysis. In combination of the morphology and element distribution, the micromorphological characteristics and component differences of the silver hare's fur glaze, gold hare's fur glaze and yellowish-brown hare's fur glaze in Shuiji kiln were discussed in the present work, which elucidated the correlation between the microstructure of  $\epsilon\text{-Fe}_2\text{O}_3$  crystals and the glaze color. This work helps in investigating the technological differences of three typical hare's fur glazes.

## Materials and methods

### Samples

The hare's fur glaze samples were unearthed in the Jian kiln relics (Shuiji, Jianyang District, Nanping City, Fujian Province), which were supposed to be belonged to Southern Song Dynasty (the 12th–13th century A.D.). The samples were numbered and grouped based on previous classification criteria [1, 4], as shown in Fig. 1. Specifically, the samples with bright shiny silver strips were grouped as silver hare's fur glaze (FJS-004 and FJS-006), the ones with golden glossy yellow strips as gold hare's fur glaze (FJS-005 and FJS-007) and the ones with yellowish-brown matte strips as yellowish-brown hare's fur glaze (FJS-008 and FJS-010). The samples were gently wiped off the dust on the surface with air-laid paper immersed with ethanol.

### The micromorphological analysis based on SEM

The MIRA3 field emission scanning electron microscope (FE-SEM, TESCAN) was applied for the micromorphological analyses of the silver, gold and yellowish-brown hare's fur glaze samples. In consideration of the rarity of samples, nondestructive analysis without coating carbon film as sample preparation was performed on the low vacuum mode. The samples were visualized by the backscattered electron (BSE) detector at the voltage of

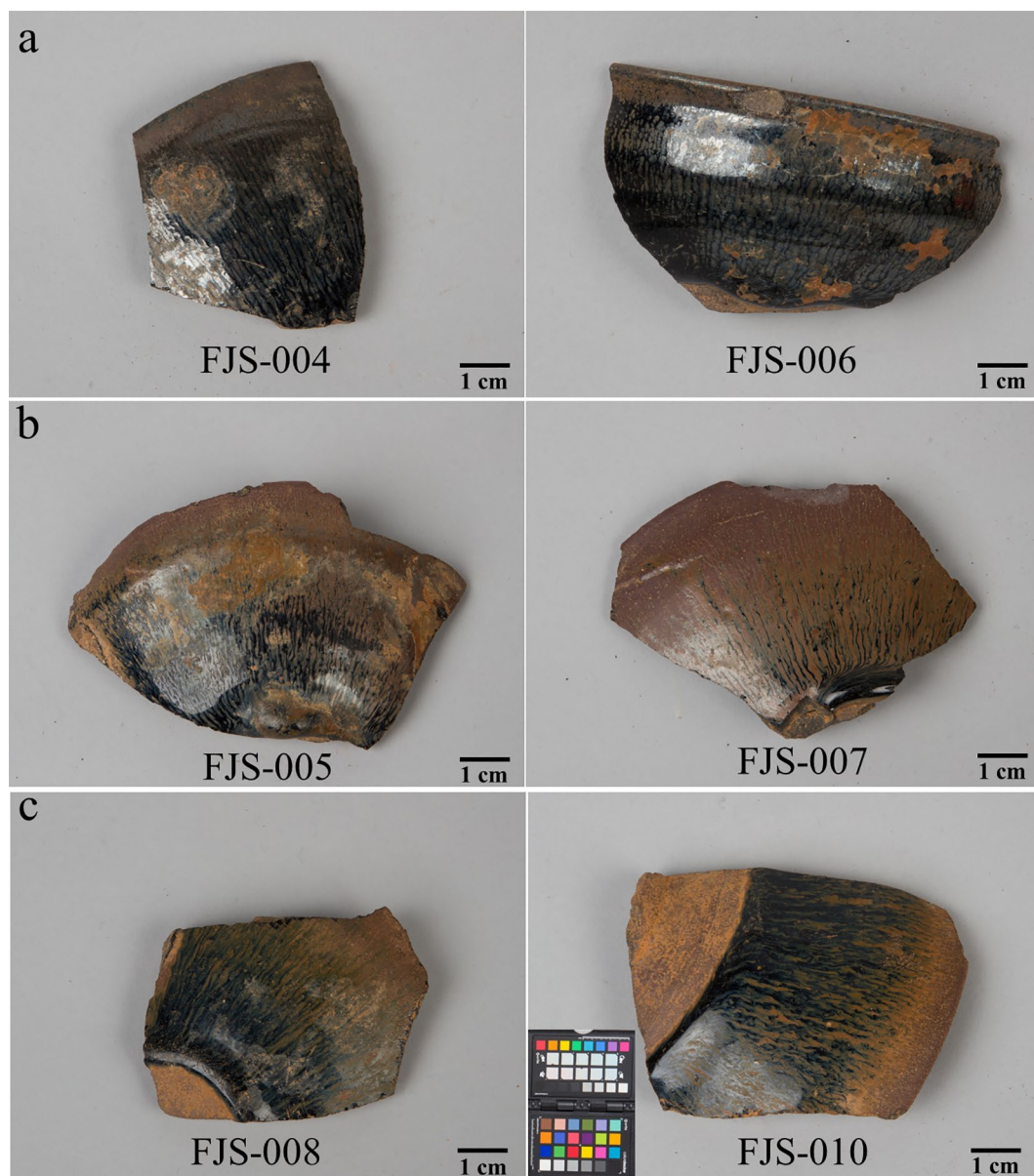


**Fig. 1** Three representative types of hare's fur glaze samples. The samples were unearthed from the Jian kiln site located at Shuiji, Jianyang District, Nanping City, Fujian Province, which were considered to be belonged to the Southern Song Dynasty. **(a)** The silver hare's fur glaze, FJS-004 and FJS-006, **(b)** the gold hare's fur glaze, FJS-005 and FJS-007, **(c)** the yellowish-brown hare's fur glaze, FJS-008 and FJS-010

20 kV and the beam intensity of 18.0, with the spot size of approximately 8 nm.

#### The elemental analysis based on EDS

The elemental imaging microanalysis and semiquantitative analysis of different types of hare's fur glaze samples were performed on EDS (Genenix, EDAX, USA) equipped with the above-mentioned SEM. The experimental conditions were set as follows: the voltage of SEM: 20 kV, BI: 18.0, spot size: 8 nm, and the measuring

time for each point: 60 s. Six strips of each sample were triply analyzed and the results were averaged for semi-quantitative analysis and were used for the three-dimensional principal component analysis (3D-PCA).

#### Results and discussion

##### The micromorphological features of three representative types of hare's fur glaze

The hare's fur area and black glaze area of the silver hare's fur glaze (FJS-004 and FJS-006), gold hare's fur glaze



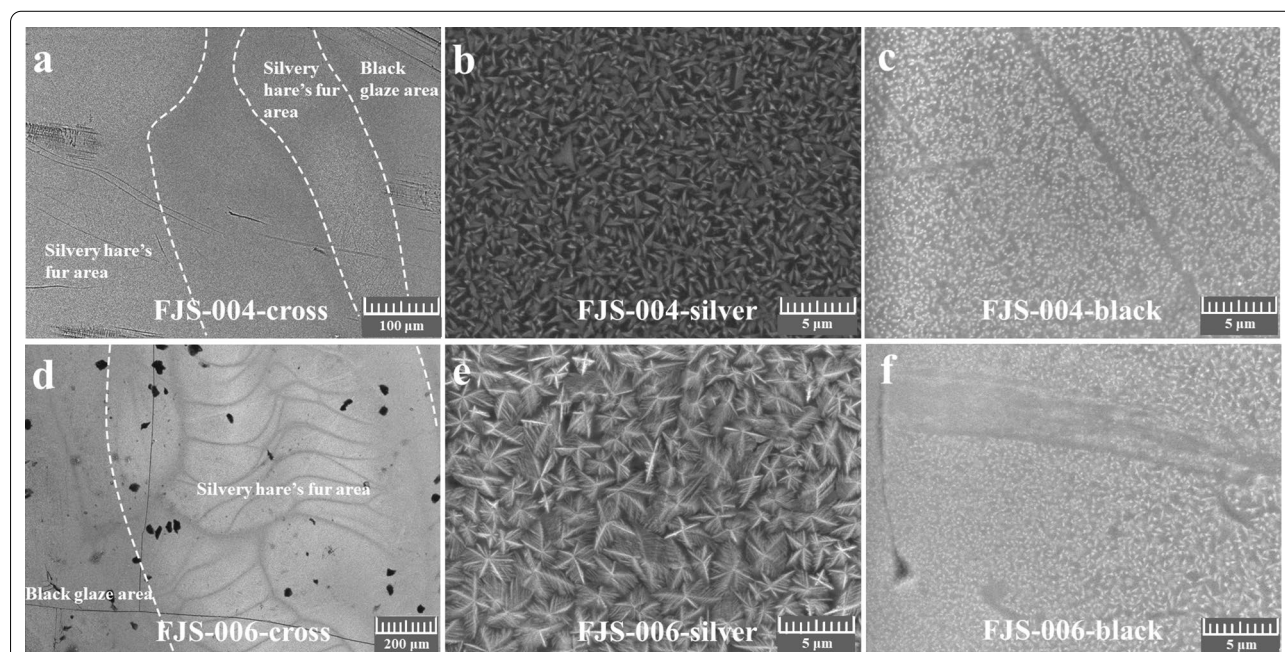
(FJS-005 and FJS-007) and yellowish-brown hare's fur glaze (FJS-008 and FJS-010) were observed, compared and characterized by SEM.

Figure 2 reveals the morphology of silvery hare's fur area and black glaze area of the silver hare's fur glaze samples. From the BSE images of the junction zones between hare's fur area and black glaze area of FJS-004 (Fig. 2a) and FJS-006 (Fig. 2d), it was indicated that the chromogenic crystals on the silvery hare's fur area were uniformly distributed and the boundaries between different areas were indistinct. The silvery hare's fur area and black glaze area were severally magnified for further analyses. The chromogenic crystals on the silvery hare's fur area were characterized by homogeneous small-sized dendritic crystals with high coverage rate on the glaze surface, of which the longest edge was approximately 1–3  $\mu\text{m}$ , as shown in Fig. 2b and 2e. Interestingly, unique crystal morphology was found on the silvery hare's fur area of FJS-004, which was supposed to be attributed to the specific orientations in crystal growth. Comparatively, the dendritic crystals in FJS-006 had 4–8 main branches, with smaller twigs on each branch. As for the black glaze areas, there were also uniformly distributed nanoscale crystals on both of the silver hare's fur glaze samples in Fig. 2c (FJS-004) and Fig. 2f (FJS-006).

The morphological features of golden hare's fur area and black glaze area of the gold hare's fur glaze samples were revealed in Fig. 3. In comparison with that of silver

hare's fur glaze, the golden hare's fur area and black glaze area of the gold hare's fur glaze samples were distinctly separated, which were represented in Fig. 3a (FJS-005) and 3d (FJS-007). In the golden hare's fur area, the distribution of chromogenic crystals was inhomogeneous, most of which were relatively uniform small-sized crystals (several microns) with sporadic single large-sized crystal (about 100  $\mu\text{m}$ ) or crystal clusters (about hundreds of microns), as displayed in Fig. 3a (FJS-005) and 3e (FJS-007). Under the higher magnification of the uniform small-sized crystals, it was observed in Fig. 3b (FJS-005) and 3f (FJS-007) that there were 4–6 main branches in the dendritic crystals with smaller twigs on each branch, the size of which was approximately 1–20  $\mu\text{m}$ . Additionally, the crystals on golden hare's fur area were featured as broad size distribution and low coverage rate in contrast to those on silver hare's fur area. Figure 3c (taking FJS-005 for example) was the BSE image of the black glaze area, in which there were no obvious crystal structures representing as amorphous materials.

In Fig. 4, the yellowish-brown hare's fur area and black glaze area of yellowish-brown hare's fur glaze samples were morphologically analyzed. The boundaries between the yellowish-brown hare's fur area and black glaze area were also unapparent, as revealed in Fig. 4a (FJS-008) and Fig. 4d (FJS-010). The yellowish-brown hare's fur area was mainly covered by amorphous iron-rich materials with honeycomb structures (Fig. 4b, taking FJS-008



**Fig. 2** The morphology of different areas of silver hare's fur glaze samples. The junctional zones between the silvery hare's fur area and black glaze area of FJS-004 (a) and FJS-006 (d), the silvery hare's fur area of FJS-004 (b) and FJS-006 (e), and the black glaze area of FJS-004 (c) and FJS-006 (f)

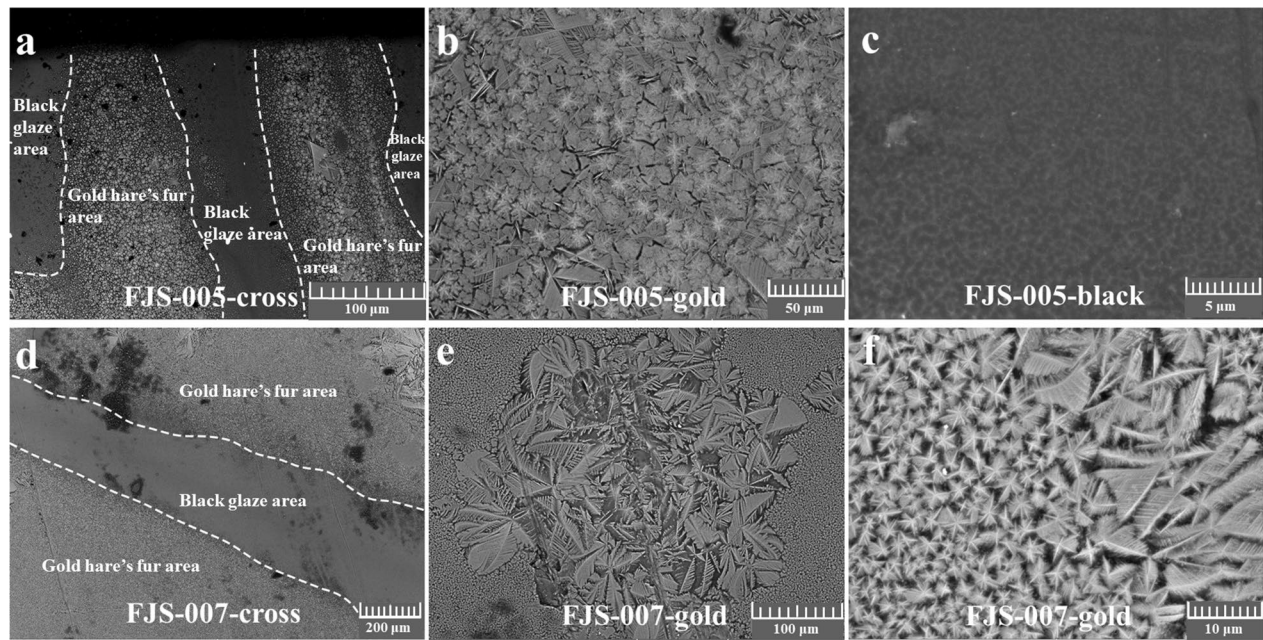


**Fig. 3** The morphological features of gold hare's fur glaze samples. The junctional zones of the golden hare's fur area and black glaze area of FJS-005 (a) and FJS-007 (d), the golden hare's fur area of FJS-005 (b) and FJS-007 (e and f), and the black glaze area of FJS-005 (c)

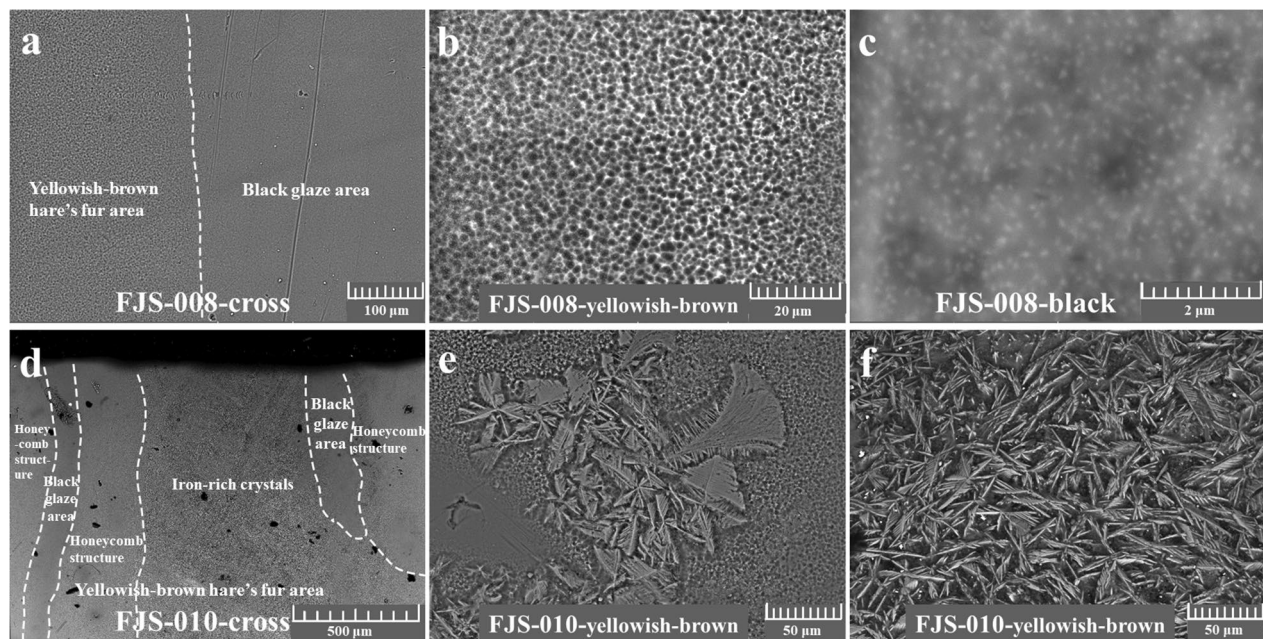


**Fig. 4** The characteristics of the morphology in yellowish-brown hare's fur glaze samples. The junctional zones of the yellowish-brown hare's fur area and black glaze area of FJS-008 (a) and FJS-010 (d), the yellowish-brown hare's fur area of FJS-008 (b) and FJS-010 (e and f), and the black glaze area of FJS-008 (c)

for example), accompanied with sporadic crystal clusters (approximately hundreds of microns, Fig. 4e, FJS-010) and large-scale feather-like dendrites (100  $\mu\text{m}$ ) at the edge of clusters. It was demonstrated in Fig. 4f (taking FJS-010 for example) that the crystals in clusters were dendrites with 4 main branches. Comparatively, the crystals sporadically deposited on the yellowish-brown hare's fur area had large inter-crystalline gaps and the lowest crystal coverage rate. In addition, it was suggested that the morphology of the black glaze area of yellowish-brown hare's fur glaze samples was similar to that of gold hare's fur glaze samples, showing as amorphous materials without apparent crystal structures, as represented in Fig. 4c taking FJS-008 for example.

Accordingly, the morphological characteristics of the hare's fur area and black glaze area of three representative types of samples were summarized as follows: [1] silver hare's fur glaze: indistinct boundaries between silvery hare's fur area and its black glaze area, dendritic and uniformly distributed crystals in silvery hare's fur area with the smallest crystal size (the longest edge of dendrites as 1–3  $\mu\text{m}$ ), highest crystal coverage on the surface, and nanoscale crystals evenly distributed on the black glaze area; [2] gold hare's fur glaze: distinct boundaries between golden hare's fur area and its black glaze area, the dendritic and inhomogeneous crystals in the golden hare's fur area, mainly small-sized crystals (the longest edge of dendrites as 1–20  $\mu\text{m}$ ) and sporadically single large-sized crystals (about 100  $\mu\text{m}$ ) or crystal clusters (about hundreds of microns) with large scale feather-like dendrites (about 50  $\mu\text{m}$ ) at the edge of clusters, relatively low crystal coverage rate, and amorphous morphology in the black glaze area; [3] yellowish-brown glaze: indistinct boundaries between yellowish-brown hare's fur area and its black glaze area, amorphous iron-rich materials with honeycomb structures in the yellowish-brown hare's fur glaze, occasionally emerged large-sized crystal clusters with feather-like dendrites (about 100  $\mu\text{m}$ ) at the edge of clusters, large inter-crystalline gaps and the lowest crystal coverage, and no obvious crystal structures in the black glaze area.

#### The elemental and crystallographic structural microanalysis of three representative types of hare's fur glaze

Based on the micromorphological analysis, the elemental distributions of silver (FJS-006), gold (FJS-005) and yellowish-brown (FJS-010) hare's fur glaze samples were imaged and semi-qualified based on SEM-EDS, which was displayed in Fig. 5.

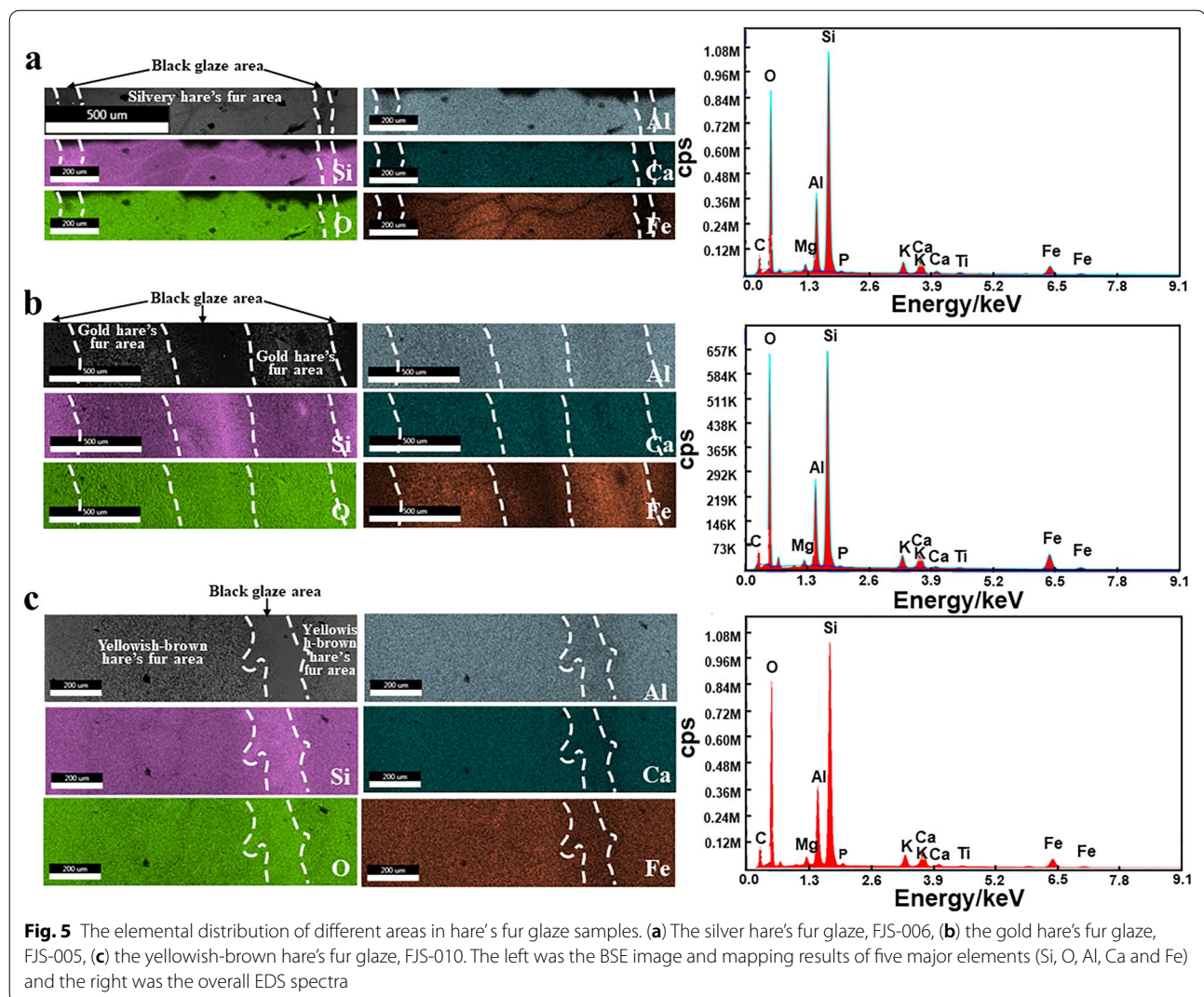
The FJS-006 sample was selected for elemental mapping analysis of the silvery hare's fur area and black glaze area, as represented in Fig. 5a. The left bottom inset was

the overall EDS spectra, indicating that the whole glaze (both the hare's fur area and black glaze area) mainly contained the following elements: Si, O, Al, Ca, Fe, K, Mg, P and Ti. The elemental distribution maps of major elements (Si, O, Al, Ca and Fe) were shown on the right, suggesting that the element contents in the silvery hare's fur area differed a lot from those in the black area. To be specific, Fe, Al and Ca were enriched in the silvery hare's fur area while Si in the black glaze area and O in both areas, manifesting that the chromogenic crystals in the silvery hare's fur area were iron oxides and the calcium oxide and aluminum oxide were originated from the raw materials of glaze, while the black glaze area were mainly  $\text{SiO}_2$ . Similar with the elemental composition and distribution of silver hare's fur glaze, the elemental results of gold hare's fur glaze and yellowish-brown hare's fur glaze were represented in Fig. 5b and 5c, respectively. In comparison of different types of hare's fur glaze samples, the elemental distribution had certain commonness, namely Fe was enriched in the hare's fur area indicating the crystals were  $\text{Fe}_2\text{O}_3$  which was in accordance with previous studies. Besides, the contents of  $\text{CaO}$  and  $\text{Al}_2\text{O}_3$  were higher in the hare's fur area than those in the black glaze area. Additionally, the black glaze of different types of glaze samples was mainly composed of  $\text{SiO}_2$ .

The semi-quantitative results of hare's fur area and black glaze area of three representative types of samples were summarized in Table 1, in which the data were normalized, averaged and denoted as the weight% of oxides. Comparing the semi-quantitative results of different areas of silver, gold and yellowish-brown hare's fur glaze, it was suggested that [1] in comparison of the hare's fur area and its black glaze area of each sample, the  $\text{Fe}_2\text{O}_3$  content differed a lot manifesting the crystals in the hare's fur glaze were  $\text{Fe}_2\text{O}_3$ , and  $\text{CaO}$  and  $\text{Al}_2\text{O}_3$  were enriched in hare's fur area which was in consistent with the mapping results. [2] When comparing the silver hare's fur glaze sample and other samples, the  $\text{SiO}_2$  content was the highest and the  $\text{Fe}_2\text{O}_3$  content the lowest in both the silvery hare's fur area and black glaze area. Considering that the concentration of crystals may affect the color, it was speculated that the low content of  $\text{Fe}_2\text{O}_3$  was related to the final appearance of silver strips in the silver hare's fur glaze. [3] In the contrastive analysis of gold hare's fur glaze and yellowish-brown hare's fur glaze samples, the  $\text{Fe}_2\text{O}_3$  content was higher and the  $\text{SiO}_2$  content was lower in the golden hare's fur area than those in the yellowish-brown area, which was supposed to be ascribed to the higher crystallinity and coverage rate of golden crystals. Besides, the black glaze areas of the two samples shared similar components which was mainly  $\text{SiO}_2$ .

The semi-quantitative results were further statistically analyzed and the three-dimensional principal component

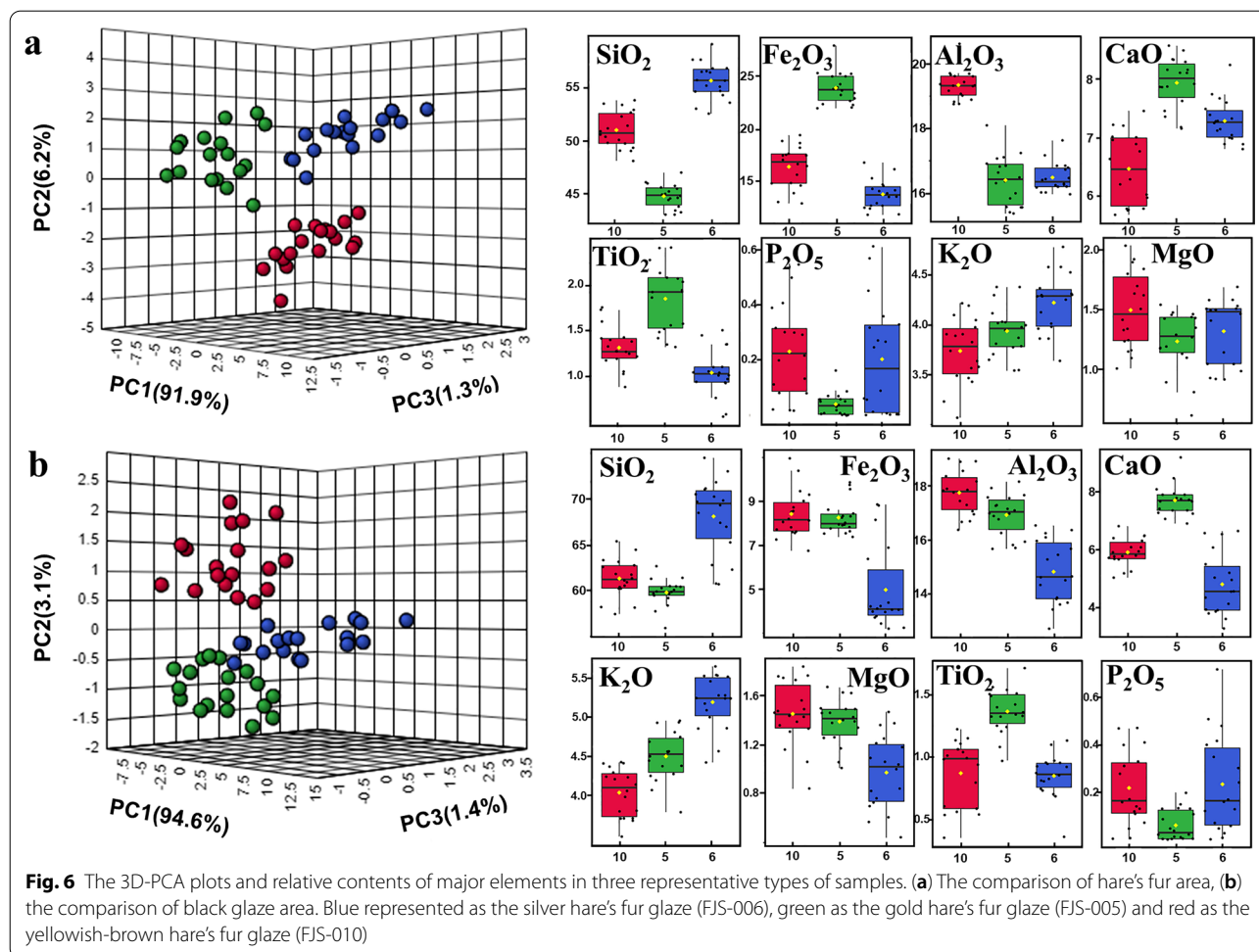


**Table 1** The semi-quantitative analyses of different areas of hare's fur glaze samples (wt%)

No.	Testing area	MgO	Al <sub>2</sub> O <sub>3</sub>	SiO <sub>2</sub>	P <sub>2</sub> O <sub>5</sub>	K <sub>2</sub> O	CaO	TiO <sub>2</sub>	Fe <sub>2</sub> O <sub>3</sub>
FJS-006	Silvery hare's fur area	1.35	16.51	55.69	0.21	4.23	7.30	1.03	13.69
	Black glaze area	0.97	14.81	68.16	0.23	5.20	4.80	0.85	4.97
FJS-005	Golden hare's fur area	1.23	16.42	44.77	0.04	3.92	7.93	1.82	23.95
	Black glaze area	1.39	16.91	59.82	0.06	4.51	7.69	1.36	8.26
FJS-010	Yellowish-brown hare's fur area	1.50	19.34	51.04	0.23	3.74	6.47	1.31	16.36
	Black glaze area	1.45	17.73	61.35	0.22	4.05	5.90	0.87	8.43

analysis (3D-PCA) plots of the hare's fur area and black glaze area were presented in Fig. 6a and 6b, respectively. In Fig. 6a, there was a great difference among the compositions of silvery, golden and yellowish-brown hare's fur areas, especially SiO<sub>2</sub>, Fe<sub>2</sub>O<sub>3</sub>, Al<sub>2</sub>O<sub>3</sub> and CaO. As for the black glaze area, the composition differences among the

three groups were much smaller than those in the hare's fur areas. The relative levels of each element of black glaze area in the three groups were similar with those in the relevant hare's fur area. For example, the content of SiO<sub>2</sub> was the highest in the silvery hare's fur area, the second highest in the yellowish-brown hare's fur area, and



the lowest in the golden hare's fur area, which was similar with the magnitude order of composition in its corresponding black glaze area.

To further identify the iron oxides with specific microstructures on three representative glazes, crystallographic structural analysis was performed on  $\mu$ -XRD and Raman spectroscopy, which were shown in Additional file 1: Figure S1. It was demonstrated that the iron-rich crystals of silver (Additional file 1: Figure S1a and 1b, FJS-006), gold (Additional file 1: Figure S1c and 1d, FJS-005) and yellowish-brown (Additional file 1: Figure S1e and 1f, FJS-010) hare's fur glazes were all  $\epsilon$ -Fe<sub>2</sub>O<sub>3</sub>, which was in consistent with previous reports [19].

From above, it could be demonstrated from the elemental mapping and semi-quantitative results that [1] the Fe<sub>2</sub>O<sub>3</sub> were enriched in the hare's fur area of all samples, manifesting that the chromogenic crystals were iron oxides. The CaO contents were also found higher in the hare's fur area than those in the corresponding black glaze area, which was considered to be related to the facilitation of Ca<sup>2+</sup> to the growth of  $\epsilon$ -Fe<sub>2</sub>O<sub>3</sub> [24] or

the promotion of anorthite (CaAl<sub>2</sub>Si<sub>2</sub>O<sub>8</sub>) or wollastonite (CaSiO<sub>3</sub>) to the migration and crystallization of iron oxides [25]. [2] For the silver hare's fur glaze sample, the SiO<sub>2</sub> content was the highest and Fe<sub>2</sub>O<sub>3</sub> the lowest in the silvery hare's fur area compared with other hare's fur areas, with relatively high-level CaO content. The elemental compositions of silver hare's fur glaze sample greatly differed from those of the other two samples. [3] For the gold hare's fur glaze sample, the Fe<sub>2</sub>O<sub>3</sub> and CaO contents were the highest and the SiO<sub>2</sub> was the lowest in the golden hare's fur area, speculating to be related to the large-scale and highly-covered  $\epsilon$ -Fe<sub>2</sub>O<sub>3</sub> on the surface of gold hare's fur glaze sample. [4] For the yellowish-brown hare's fur glaze sample, the Al<sub>2</sub>O<sub>3</sub> content was the highest with the relatively low-level CaO, which was considered to be attributed to the poor crystallinity of  $\epsilon$ -Fe<sub>2</sub>O<sub>3</sub> on the sample. [5] For all the black glaze areas, the compositional magnitude order was in consistent with that of the corresponding hare's fur area. The elemental results revealed the chemical compositional differences in three representative hare's fur



**Table 2** The morphological features and compositional differences of hare's fur samples

Type	Morphological features	Compositional differences
Silver hare's fur glaze	(1) Indistinct boundaries (2) Silvery hare's fur area: dendritic, uniformly-distributed, small-sized and highly-covered $\epsilon$ -Fe <sub>2</sub> O <sub>3</sub> crystals (3) Black glaze area: evenly distributed nanoscale crystals	(1) The highest SiO <sub>2</sub> in all areas (2) The lowest Fe <sub>2</sub> O <sub>3</sub> in all areas (3) Relatively high-level CaO in hare's fur area
Gold hare's fur glaze	(1) Distinct boundaries (2) Golden hare's fur area: dendritic, inhomogeneous and relatively low-covered crystals, mainly small-sized crystals and sporadically single large-sized crystals or crystal clusters with large scale feather-like dendrites at the border (3) Black glaze area: no obvious crystals	(1) The highest Fe <sub>2</sub> O <sub>3</sub> in the hare's fur area (2) The lowest SiO <sub>2</sub> in all areas (3) The highest CaO in all areas
Yellowish-brown hare's fur glaze	(1) Indistinct boundaries (2) Yellowish-brown hare's fur area: amorphous iron-rich materials with honeycomb structures, occasionally emerged large-sized crystal clusters with feather-like dendrites at the margin, large inter-crystalline gaps with the lowest crystal coverage (3) Black glaze area: no obvious crystal structures	(1) The highest Al <sub>2</sub> O <sub>3</sub> in all areas (2) The relative low-level of CaO in the hare's fur area

glazes, which may contribute to the further interpretation of the coloration and technical differences. It was speculated that relative low-level of Fe<sub>2</sub>O<sub>3</sub>, high-level of SiO<sub>2</sub> and CaO may relate to the formation of  $\epsilon$ -Fe<sub>2</sub>O<sub>3</sub> with silvery hues, while high-level of Fe<sub>2</sub>O<sub>3</sub> and CaO and low-level of SiO<sub>2</sub> were connected with the gold  $\epsilon$ -Fe<sub>2</sub>O<sub>3</sub>. Nevertheless, high-level of Al<sub>2</sub>O<sub>3</sub> may inhibit the crystallization of  $\epsilon$ -Fe<sub>2</sub>O<sub>3</sub>, leading to the amorphous  $\epsilon$ -Fe<sub>2</sub>O<sub>3</sub> with honeycomb structures.

Collectively, the morphological features and compositional differences of three types of hare's fur glaze samples were summarized in Table 2.

## Conclusions

In conclusion, the silver, gold and yellowish-brown hare's fur glaze samples were compared based on typology from the morphological and compositional aspects. The morphological features and compositional differences of three representative types of samples were summarized, demonstrating the differences in the size, distribution and coverage of crystals and the distribution and contents of materials. Our work may contribute to the further explanation of technological differences of three hare's fur glazes. However, further validations should be performed using more hare's fur samples since our study was carried out based on a small number of samples.

## Supplementary Information

The online version contains supplementary material available at <https://doi.org/10.1186/s40494-021-00498-0>.

**Additional file 1: Figure S1.** The crystallographic structural analysis of the iron oxides on three representative glazes based on  $\mu$ -XRD and Raman spectroscopy.

## Acknowledgements

The authors appreciated the help of Hanwen Liu from the Palace Museum and TESCAN Co. (China) and EDAX Co. (China) for the assistance of instrument operation. We also thank Guanqun Luo from Jianyang City Museum for providing the hare's fur glaze samples.

## Authors' contributions

MG, designing and performing the experiments; analyzing data; writing. BK, grouping the hare's fur glaze samples and analyzing data. XW: funding acquisition; writing-review and editing. GL, performing the experiments and analyzing data. CJ, performing the experiments and analyzing data. HL, grouping the hare's fur glaze samples and analyzing data. YD, grouping the hare's fur glaze samples and analyzing data. YL: conceiving and designing the experiments; providing resources; writing-review and editing. All authors read and approved the final manuscript. Xiangjun Wei: funding acquisition; writing-review and editing.

## Funding

This work was supported by National Natural Science Foundation of China (NSFC) (No. U1932203 and U1832164) and SSRF.

## Availability of data and materials

The data in the current study are available from the corresponding author on reasonable request. Baoqiang Kang, grouping the hare's fur glaze samples and analyzing data.

## Competing interests

The authors declare no competing financial interests.

Received: 1 December 2020 Accepted: 8 February 2021

Published online: 17 February 2021

## References

- Li J. History of Science technology in china ceramic volume. Beijing: Beijing Science Press; 1998.
- Mowry RD, Farrell E, Rousmaniere NC, Arthur M. Hare's Fur, Tortoiseshell and Partridge Feathers: Chinese Brown- and Black-Glazed Ceramics, 400–1400: Harvard University Art Museums; 1996.
- Li M, Li W, Lu X, Xu C. Controllable Preparation and decorative effect of iron-based crystalline glazes. *J Chin Ceram Soc.* 2020;48:1134–44.
- Chen X, Chen S, Huang R, Zhou X, Ruan M. A Study on song dynasty jian bowl. *Chin Ceram.* 1983;2:61–9 (in Chinese).
- Colomban PH, Sagon G, Huy LQ, Liem NQ, Mazerolles L. Vietnamese (15th Century) blue-and-white, tam thai and lustre porcelains/stonewares:

- glaze composition and decoration techniques. *Archaeometry*. 2004;46(1):125–36.
6. Kusano Y, Fukuhara M, Takada J, Doi A, Ikeda Y, Takano M. Science in the art of the master Bizen potter. *Acc Chem Res*. 2010;43(6):906–15.
  7. Li X, Lu J, Yu X, Zhou J, Li L. Imitation of ancient black-glazed Jian bowls (Yohen Tenmoku): Fabrication and characterization. *Ceram Int*. 2016;42(14):15269–73.
  8. Shi P, Wang F, Zhu J, Zhang B, Zhao T, Wang Y, et al. Effect of phase separation on the Jian ware blue colored glaze with iron oxide. *Ceram Int*. 2018;44(14):16407–13.
  9. Tuček Ji, Zbořil R, Namai A, Ohkoshi S. -i.  $\epsilon$ -Fe<sub>2</sub>O<sub>3</sub>: an advanced nanomaterial exhibiting giant coercive field, millimeter-wave ferromagnetic resonance, and magnetoelectric coupling. *Chem Mater*. 2010;22(24):6483–505.
  10. Xu Y, Qin Y, Ding F. Characterization of the rare oil spot glazed bowl excavated from the Xiaozhou kiln site of north China. *Ceram Int*. 2017;43(12):8636–42.
  11. Wen R, Wang D, Wang L, Dang Y. The colouring mechanism of the Brown glaze porcelain of the Yaozhou Kiln in the Northern Song Dynasty. *Ceram Int*. 2019;1:10589–95.
  12. Hoo Q, Liang Y, Yan X, Wang X, Tiewa C, Cao X. Millimeter-sized flower-like clusters composed of mullite and  $\epsilon$ -Fe<sub>2</sub>O<sub>3</sub> on the Hare's Fur Jian Ware. *J Eur Ceram Soc*. 2020;40:4340–7.
  13. Simsek Franci G, Akkas T, Yildirim S, Yilmaz S, Birdevrim AN. Characterization of a Jian-like sherd with the optical microscope, confocal Raman, wavelength-dispersive X-ray fluorescence, and portable XRF spectrometers. *J Raman Spectrosc*. 2020;51(8):1343–52.
  14. Jin J, Ohkoshi S, Hashimoto K. Giant coercive field of nanometer-sized iron oxide. *Adv Mater*. 2004;16(1):48–51.
  15. Bukhtiyarova GA, Shuvaeva MA, Bayukov OA, Yakushkin SS, Martyanov ON. Facile synthesis of nanosized  $\epsilon$ -Fe<sub>2</sub>O<sub>3</sub> particles on the silica support. *J Nanopart Res*. 2011;13(10):5527–34.
  16. Taboada E, Gich M, Roig A. Nanospheres of silica with an epsilon-Fe<sub>2</sub>O<sub>3</sub> single crystal nucleus. *Acs Nano*. 2009;3(11):3377.
  17. Shen B, Sciau P, Wang T, Brunet M, Li J, Lu W, et al. Micro-structural study of colored porcelains of Changsha kiln using imaging and spectroscopic techniques. *Ceram Int*. 2018;44(15):18528–34.
  18. Wang L, Wang Y, Zhang M, Li Q, Wu J, Liu Z, et al. Three-dimensional microstructure of epsilon-Fe<sub>2</sub>O<sub>3</sub> crystals in ancient Chinese sauce glaze porcelain revealed by focused ion beam scanning electron microscopy. *Anal Chem*. 2019;91(20):13054–61.
  19. Dejoie C, Sciau P, Li W, Noé L, Mehta A, Chen K, et al. Learning from the past: Rare  $\epsilon$ -Fe<sub>2</sub>O<sub>3</sub> in the ancient black-glazed Jian (Tenmoku) wares. *Sci Rep*. 2014;4(1):4941.
  20. Li W, Luo H, Li J, Li J, Guo J. Studies on the microstructure of the black-glazed bowl sherds excavated from the Jian kiln site of ancient China. *Ceram Int*. 2008;34(6):1473–80.
  21. Changsong X, Weidong L, Xiaoke L, Wenjiang Z, Hongjie L, Jingkun G. Unveiling the science behind the tea bowls from the Jizhou kiln. Part II. microstructures and the coloring mechanism. *Ceram Int*. 2018; 1: 19461–73.
  22. Liu Z, Jia C, Li L, Li X, Ji L, Wang L, et al. The morphology and structure of crystals in Qing Dynasty purple-gold glaze excavated from the Forbidden City. *J Am Ceram Soc*. 2018;101(11):5229–40.
  23. Li WD, Zhang W, Lu XK, Zheng NZ, Luo HJ. Chemical compositions and microstructures of hare's fur black-glazed porcelains from Jian kiln, Jizhou kiln and Yaozhou kiln sites. *J Build Mater*. 2011;14:329–34.
  24. Ohkoshi S-i, Sakurai S, Jin J, Hashimoto K. The addition effects of alkaline earth ions in the chemical synthesis of  $\epsilon$ -Fe<sub>2</sub>O<sub>3</sub> nanocrystals that exhibit a huge coercive field. *J Appl Phys*. 2005;97(10):10k312.
  25. Reedy C. Petrographic. and image analysis of thin sections of classic wares of song dynasty. *Proceedings of International symposium on science and technology of five great wares of the song dynasty*. Beijing: Science Press; 2016. p. 381–90.

## Publisher's note

Springer Nature remains neutral with regard to jurisdictional claims in published maps and institutional affiliations.

**Submit your manuscript to a SpringerOpen<sup>®</sup> journal and benefit from:**

- Convenient online submission
- Rigorous peer review
- Open access: articles freely available online
- High visibility within the field
- Retaining the copyright to your article

---

Submit your next manuscript at ► [springeropen.com](https://www.springeropen.com)